

Effect of Grain Refinement on Strength and Ductility in Dual-Phase Steels

Marion Calcagnotto^{1*}, Dirk Ponge¹, Yoshitaka Adachi² and Dierk Raabe¹

¹Max-Planck-Institut für Eisenforschung GmbH, Max-Planck-Straße 1, 40237 Düsseldorf, Germany

²National Institute for Materials Science, 1-2-1 Sengen, Tsukuba 305-0047, Japan

*E-mail: m.calcagnotto@mpie.de

Abstract: Large strain warm deformation at different temperatures and subsequent intercritical annealing has been applied to obtain fine grained (FG, 2.4 μm) and ultrafine grained (UFG, 1.2 μm) ferrite/martensite dual-phase (DP) steels. Their mechanical properties were tested under tensile conditions and compared to a hot deformed coarse grained (CG, 12.4 μm) counterpart. Both yield strength and tensile strength follow a Hall-Petch type linear relationship, whereas uniform elongation and total elongation are hardly affected by grain refinement. The initial strain hardening rate as well as the reduction in area increase with decreasing grain size. The deformation and fracture behavior of the steels were analyzed using scanning electron microscopy (SEM) combined with electron backscatter diffraction (EBSD). Slip band evolution was studied by multistep tensile tests. The increase in strength at improved ductility is explained with the enhanced martensite plasticity as a result of plastic constraints in UFG ferrite and the delayed formation of voids and martensite particle cracks due to the more homogeneous distribution and more spherical shape of UFG martensite particles.

1. INTRODUCTION

Dual-phase (DP) steels consisting of a soft ferrite matrix and typically 5-30 vol.-% of hard martensite particles combine high strength with good formability and weldability. Therefore, they are widely used for automotive applications [1]. Since their development three decades ago, the microstructure-property relationships have been extensively studied [2]. In view of the increasing demands for occupant safety and fuel efficiency, further strengthening of DP steels without a loss in ductility is required. Grain refinement is a promising method to achieve this aim [3-7]. In recent years, a variety of new processing routes has been developed to produce ultrafine grained (UFG) low carbon steels with a ferrite grain size of 1 μm and below [8]. UFG DP steels have been produced by applying a two-step processing route consisting of 1) a deformation treatment to produce UFG ferrite and finely dispersed cementite or pearlite and 2) a short intercritical annealing in the ferrite/austenite two-phase field followed by quenching to transform all austenite into martensite. Grain refinement in step 1) was achieved by severe plastic deformation [5] or advanced thermomechanical processing routes [6,7,9]. It was consistently found that yield strength and tensile strength are increased due to grain refinement, whereas uniform and total elongation are less affected. The strain hardening rate was found to increase with decreasing grain size [5] which is in contrast to the observation of the very restricted strain hardening rate in UFG low carbon ferrite/cementite steels [10]. As the number of investigations is very limited, further research is necessary to understand the mechanical response of DP steels to ferrite grain sizes close to or below 1 μm . The aim of the present study is to shed new light on the deformation and fracture mechanisms in a CG, FG and an UFG DP steel. In conjunction with tensile data, the microstructure evolution during deformation and the fracture mechanisms were studied by using SEM and high-resolution EBSD.

2. EXPERIMENTAL PROCEDURES

The chemical composition of the steel used was 0.17 C, 1.49 Mn, 0.22 Si, 0.033 Al, 0.0033 N, 0.0017 P and 0.0031 S (in wt.%). The steel was produced by vacuum induction melting. Samples (50x40x60 mm³) were machined directly from the cast ingot. The thermomechanical processing was realized by use of a large scale 2.5 MN hot press located at the Max-Planck-Institut für Eisenforschung [11]. Austenitization at 934°C for 3 min and subsequent deformation at the same temperature produces fully recrystallized austenite which transforms into relatively coarse grained (CG) ferrite and pearlite upon slow cooling (CG-route). Grain refinement is achieved by subsequent warm deformation exerting a four-step flat compression series with a strain of 0.4 per step, an interpass time of 0.5 s and a strain rate of 10 s⁻¹. The deformation temperature controls the degree of grain refinement. At 700°C, a fine grained (FG) ferrite matrix is obtained with small islands of pearlite and globular cementite (FG-route). At 550°C, the ferrite is refined to around 1 μm which is referred to as UFG ferrite. The pearlite is completely replaced by spheroidized sub- μm sized cementite which is distributed homogeneously along the ferrite grain boundaries (UFG-route). All specimens were then subjected to 3 min intercritical annealing at 730°C in a salt bath furnace, followed by water quenching to obtain a ferrite/martensite DP structure with around 30 vol.% martensite.

Round tensile test specimens with a diameter of 4 mm and a gage length of 20 mm were machined according to the German Industry Norm DIN 50125-B. Tensile tests were conducted at room temperature with a constant cross-head speed of 0.5 mm/min. Three tensile tests were performed for each material. Samples for SEM and EBSD were prepared by standard metallographic grinding and polishing methods. Samples for SEM observations were additionally etched for 2 sec in 1% Nital. Ferrite grain size and martensite volume fraction were determined from a range of SEM images

by the mean linear intercept method and the point counting method, respectively. EBSD experiments were conducted using a JEOL JSM 6500F high-resolution SEM equipped with field emission gun (FEG). Data analysis was done using the TSL OIM software package [12]. To study slip band evolution during deformation, some additional tensile tests were conducted which were interrupted at different strain levels. The plastic strain in the region of interest was determined by measuring the distance of two hardness indents after each straining step.

3. RESULTS

The microstructure obtained after hot deformation and air cooling followed by intercritical annealing (CG-route) consists of a ferrite matrix with a grain size of 12.4 μm (d_f) and 31.3 % martensite (f_m) (Fig. 1, Table 1), the latter occurring as isolated particles and as aligned bands in equal shares. By applying multi-pass warm deformation at 700°C (FG-route) and 550°C (UFG-route) between hot deformation and intercritical annealing, the ferrite grain size is reduced to 2.4 μm and 1.2 μm , respectively. The martensite fraction is 30.1 vol.-% in the FG-steel and 29.8 vol.-% in the UFG-steel.

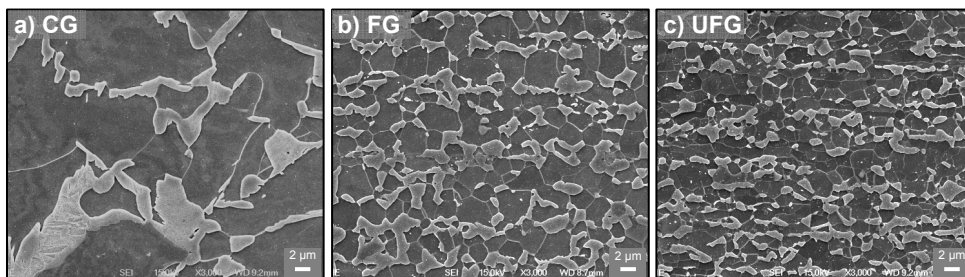


Fig. 1. Micrographs of the three steels investigated, varying only in the grain size.

Figure 2 shows the engineering stress-strain curves of the CG, FG and UFG steels. They all show the typical behavior of as-quenched ferrite/martensite DP steels: low elastic limit, absence of a distinct yield point, continuous yielding and high initial strain hardening rate. These features have been attributed to residual stresses and dislocation heterogeneities present in the ferrite as result of the austenite-to-martensite transformation [13-15]. With decreasing grain size, yield strength ($\sigma_{0.2}$) and tensile strength (TS) are remarkably increased. The yield ratio (YR) is nearly constant (Table 1). The uniform elongation (ϵ_u) varies slightly around 7% for the CG, FG and UFG steels. Both total elongation (ϵ_t) and reduction in area (RA) are highest in the FG steel. The UFG steel has a lower total elongation than the CG steel, but a higher reduction in area. However, the differences are rather small. The initial strain hardening rate is

Table 1. Microstructural and mechanical parameters.

	f_m (%)	d_f (μm)	$\sigma_{0.2}$ (MPa)	TS (MPa)	YR	ϵ_u (%)	ϵ_t (%)	RA (%)	n (2-5%)
CG	31.3	12.4	445	870	0.51	7.2	7.7	13.0	0.24
FG	30.1	2.4	483	964	0.50	7.4	8.9	18.7	0.22
UFG	29.8	1.2	525	1037	0.51	7.1	7.3	15.3	0.21

increased by grain refinement, but is nearly the same for the FG and the UFG steel. At higher strain levels, strain hardening rate is almost equal for all specimen. The n-value calculated at strain levels between 2% and 5% (Table 1) drops off slightly from 0.24 to 0.21 with decreasing grain size.

The inserted micrographs in Fig. 2 reveal the respective fracture modes of the steels. In case of the CG steel, it is mainly brittle, which is documented by well-defined facets and river patterns in ferrite cleavage planes. Martensitic areas consist of dimples. The dominant fracture mode of the FG steel is ductile, although smaller parts of the specimen have undergone brittle fracture. The UFG steel shows dimples throughout the specimens. This suggests a failure process of void nucleation and growth and hence, entirely ductile fracture. Some dimples are formed around inclusions. To find out the preferred void nucleation sites, surfaces perpendicular to the fracture surface were also observed. In the CG steel, the main fracture mechanism is martensite particle cracking. The cracks form mostly in the banded areas perpendicular to the applied tensile strain. Void nucleation and growth along ferrite/martensite interfaces occurs to a lesser extent within the areas of isolated martensite islands. For the other steels, the voids form primarily at ferrite/martensite interfaces and are distributed more homogeneously. Martensite particle cracking takes place in particles which exceed the average martensite particle size and occurs only after necking.

The microstructure evolution during deformation is exemplarily illustrated for the CG and the UFG steel as the FG steel shows an intermediate deformation behavior. Figure 3 shows Image Quality maps of EBSD scans taken perpendicular to the fracture surface of the tensile specimen. Fig. 3a,b show the CG steel in the area of uniform elongation (a) and close to neck (b). Fig. 3c,d illustrate the respective areas in the UFG steel. Martensite is easily identified by its lower Image Quality and the particle subdivision into blocks or packets. In the CG steel, strain localization in ferrite was observed after straining to the uniform elongation (~7%), as indicated by arrows 1). Martensite particle cracking was observed in some

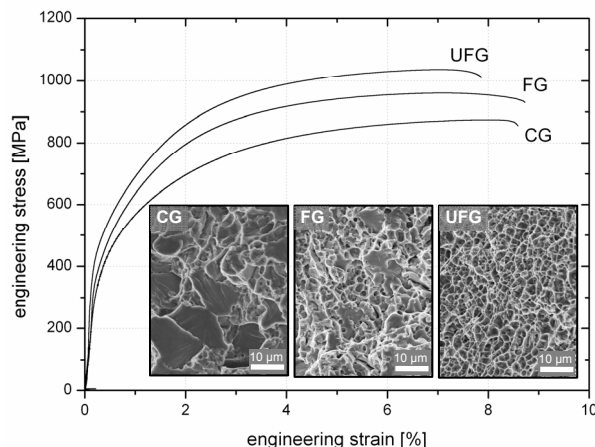


Fig. 2. Mechanical properties and fracture surfaces.

areas, arrow 2). In contrast, the UFG steel shows a less pronounced substructure formation in ferrite. Instead, the martensite shows considerable plastic deformation and is elongated in the tensile direction together with the ferrite, arrows in Fig. 3c). After failure, strain localization and subgrain formation of the CG ferrite is intense, particularly close to ferrite/martensite interfaces. Martensite particle cracking and interface decohesion is numerous in this state, arrows in Fig. 3b). In the UFG steel (Fig. 3d), it can be easily seen that martensite is extensively deformed and elongated in the tensile direction. Compared to the CG steel, the deformation substructure in ferrite is less well developed, i.e. ferrite has accommodated less plastic strain by developing a dislocation cell structure than in the CG steel. Moreover, the distribution of the deformation substructure within the ferrite grains is more homogeneous than in the CG structure. Voids form mainly along the ferrite/martensite interface (arrows in Fig. 3d) and are also elongated in the tensile direction.

4. DISCUSSION

In general, the enhancement in strength due to grain refinement is accompanied by a deterioration of ductility. However, it was shown in previous studies [3-7] that this does not apply to DP steels. Instead, it was shown, that uniform and total elongation are only slightly affected by a decreasing ferrite grain size, as it is also observed in the present study. This was explained with the increase in strain hardening rate with decreasing grain size [4,5,16] that leads to a nearly unchanged uniform elongation.

Martensite plasticity is an important factor controlling the overall deformation behavior of DP steels. By deforming, martensite releases part of the local stress concentrations and retards failure which results in higher fracture strains. The martensite in the CG steel remains in the elastic state even in the necked area of the tensile specimen. On the other hand, the FG and UFG steel clearly show considerable martensite deformation before the onset of necking. To find out the reason for martensite plasticity in the UFG steel, one has to take a look at the slip band formation mode. In the CG steel, the slip bands appear wavy, are strongly intersecting and do not show preferred orientation after 3.4% plastic strain (Fig. 4a). In contrast, the UFG ferrite shows basically two sets of nearly planar slip bands which are oriented around 40° to the tensile direction after 2.9% plastic strain (Fig. 4b). This suggests that plastic deformation is constrained in the UFG ferrite. Planar and wavy slip mode in DP steels was reported by Tomota [17]. The author explains the occurrence of planar slip with the restricted operation of plastic relaxation of strain incompatibility while the wavy slip mode is associated with active plastic relaxation. Plastic relaxation can be realized by 1) additional plastic flow in the softer phase, 2) onset of plastic flow in the harder phase or 3) fracture of the harder phase or decohesion at the interface [17]. In the CG steel, plastic relaxation can take place by strain localization and subgrain formation in ferrite and by martensite particle cracking (Fig. 3b). Therefore, slip bands develop in a wavy mode (Fig. 4a). However, the finer the ferrite grain size the more difficult becomes the plastic deformation of ferrite due to restricted formation of dislocation pile-ups. Due to the nearly spherical shape and the resulting high toughness of martensite particles, both interface decohesion and particle cracking are impeded at low strains. Therefore, we observe planar slip mode (Fig. 4b). At later stages of plastic deformation ($>3\%$), plastic relaxation in the UFG steel occurs by the onset of martensite plastic flow and by interface decohesion (Fig. 3d). Hence, the plasticity of martensite is strongly dependent on the plastic constraints in ferrite. The plastic constraint imposed on UFG ferrite is partly balanced by the more spherical morphology of UFG martensite compared to the CG martensite, which often covers ferrite grain boundaries or appears as stringers. At a constant particle volume fraction, the spherical shape toughens the martensite particles and increases the ductility of the composite. Therefore, the UFG steel shows a ductility comparable to the CG at much higher strength levels steel due to the advantageous morphology and distribution of martensite and the plastic deformability of martensite as a response to the restricted plasticity in ferrite.

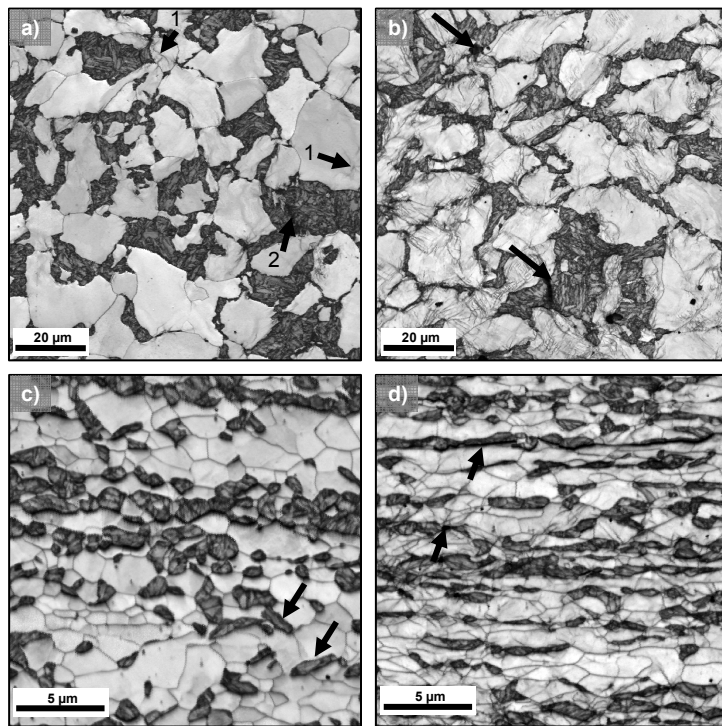


Fig. 3. Microstructure evolution during tensile straining in CG (a,b) and UFG (c,d) in the area of uniform elongation (~7% a,c) and close to the neck (b,c). Rolling and tensile direction are horizontal.

the UFG steel occurs by the onset of martensite plastic flow and by interface decohesion (Fig. 3d). Hence, the plasticity of martensite is strongly dependent on the plastic constraints in ferrite. The plastic constraint imposed on UFG ferrite is partly balanced by the more spherical morphology of UFG martensite compared to the CG martensite, which often covers ferrite grain boundaries or appears as stringers. At a constant particle volume fraction, the spherical shape toughens the martensite particles and increases the ductility of the composite. Therefore, the UFG steel shows a ductility comparable to the CG at much higher strength levels steel due to the advantageous morphology and distribution of martensite and the plastic deformability of martensite as a response to the restricted plasticity in ferrite.

The increased ductility due to grain refinement is reflected in the fracture mechanisms of the steels. At room temperature, the UFG steel shows ductile fracture mechanisms, the CG steel shows mainly brittle behavior and the FG steel exhibits an intermediate fracture mechanism. The brittle fracture behavior is favored due to martensite banding, large martensite particle size and unfavorable distribution along ferrite grain boundaries in the CG steel. Near the

martensite bands, the local stress concentrations are highest as the stress relaxation by deformation of adjacent ferrite grains is restricted. As the plasticity of martensite is very low, premature martensite cracking or void nucleation at the interface occurs. Moreover, it is possible that the banded martensite contains more carbon than the isolated martensite due to Mn segregation which acts as a sink for carbon. Therefore, it is likely that the banded martensite is less deformable and undergoes brittle fracture more easily. As a consequence, premature martensite cracking controls both tensile strength and uniform elongation in the CG steel. The fractured martensite acts as a sharp notch [18], leading to cleavage in the ferrite. In the present case, martensite cracks are stopped by the ferrite in the CG steel but penetrate deeper into the ferrite grain with increasing strain. Close to the tensile strength, plastic constraints are too high to impede the crack penetration, and ferrite fails by cleavage. In the other steels, martensite particle cracking is less frequent and does not lead to ferrite cleavage fracture. As the stress at the crack tip increases with the reciprocal root of its size and its size is restricted by the grain diameter, grain refinement increases the cleavage fracture stress. Therefore, cleavage fracture is inhibited when grain size is reduced. The toughening effect is due to the refinement of both ferrite and martensite, as the effective grain size in martensite (the coherent length of $\{001\}$ plane in martensite packet) is also reduced. Moreover, the plastic strain needed for the failure of a particle increases with decreasing particle size. This is commonly explained by the smaller number of dislocations piling-up at a grain or phase boundary. As the shear stress at the head of a pile-up increases linearly with the number of dislocations, the local stress concentrations at grain boundaries will be reduced and therefore, crack nuclei will be less.

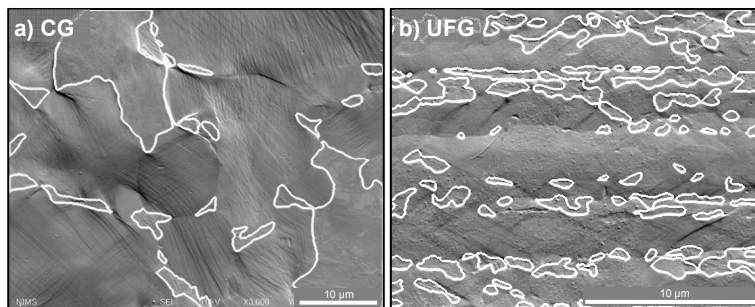


Fig. 4. Wavy slip band formation in CG after 3.4% plastic strain (a) and planar slip band arrays in UFG after 2.9% plastic strain (b). Rolling and tensile direction are horizontal. Martensitic areas are encircled.

The fractured martensite acts as a sharp notch [18], leading to cleavage in the ferrite. In the present case, martensite cracks are stopped by the ferrite in the CG steel but penetrate deeper into the ferrite grain with increasing strain. Close to the tensile strength, plastic constraints are too high to impede the crack penetration, and ferrite fails by cleavage. In the other steels, martensite particle cracking is less frequent and does not lead to ferrite cleavage fracture. As the stress at the crack tip increases with the reciprocal root of its size and its size is restricted by the grain diameter, grain refinement increases the cleavage fracture stress. Therefore, cleavage fracture is inhibited when grain size is reduced. The toughening effect is due to the refinement of both ferrite and martensite, as the effective grain size in martensite (the coherent length of $\{001\}$ plane in martensite packet) is also reduced. Moreover, the plastic strain needed for the failure of a particle increases with decreasing particle size. This is commonly explained by the smaller number of dislocations piling-up at a grain or phase boundary. As the shear stress at the head of a pile-up increases linearly with the number of dislocations, the local stress concentrations at grain boundaries will be reduced and therefore, crack nuclei will be less.

5. CONCLUSIONS

Three low carbon dual-phase steels with nearly constant martensite fraction around 30 vol.-% and different ferrite grain size were produced by applying hot deformation and large strain warm deformation at different deformation temperatures. Their deformation and fracture mechanisms were studied based on tensile data and microstructure observations. The main conclusions are:

1. Grain refinement leads to an increase of both yield strength and tensile strength. Uniform elongation and total elongation are hardly affected. Initial strain hardening rate and reduction in area increase as the grain size decreases.
2. Grain refinement promotes the formation of planar slip band arrays, whereas wavy slip bands are developed in the CG steel. This was explained by plastic constraints being present in UFG ferrite. The wavy slip mode leads to pronounced lattice rotations and early formation of a subgrain structure in CG ferrite. The planar slip mode forces martensite to deform plastically earlier during plastic deformation, whereas strain localization and subgrain formation is impeded in UFG ferrite.
3. The increase in strength at constant ductility due to grain refinement is attributed to the enhanced plasticity of martensite.
4. Grain refinement promotes ductile failure behavior. The formation of martensite particle cracks and cleavage fracture in ferrite is suppressed in the FG and UFG steels due to the more homogeneous distribution, smaller size and more spherical shape of martensite particles.

REFERENCES

- [1] K. Hulka: Mater. Sci. Forum, 414-415(2003), 101.
- [2] M. S. Rashid: Annu. Rev. Mater. Sci., 11(1981), 245.
- [3] P. H. Chang and A. G. Preban: Acta Metall., 33(1985), 897.
- [4] Z. Jiang, Z. Guan and J. Lian: Mater. Sci. Eng. A, 190(1995), 55.
- [5] Y. Son, Y. K. Lee, K.-T. Park, C. S. Lee and D. H. Shin: Acta Mater., 53(2005), 3125.
- [6] P. Tsipouridis, E. Werner, C. Kremaszky and E. Tragl: Steel Res. Int., 77(2006), 654.
- [7] K. Mukherjee, S. Hazra, P. Petkov and M. Militzer: Mater. Manuf. Processes, 22(2007), 511.
- [8] R. Song, D. Ponge, D. Raabe, J. G. Speer and D. K. Matlock: Mater. Sci. Eng. A, 441(2006), 1.
- [9] M. Calcagnotto, D. Ponge and D. Raabe: ISIJ Int., 48(2008), 1096.
- [10] N. Tsuji, Y. Ito, Y. Saito and Y. Minamino: Scripta Mater., 47(2002), 893.
- [11] R. Kaspar and O. Pawelski: Materialprüfung, 31(1989), 14.
- [12] D. Dingley: J. Microsc., 213(2004), 214.
- [13] G. R. Speich and R. L. Miller. In: R.A. Kot and J.W. Morris, editors. Structure and Properties of Dual-Phase Steels, New York (NY): The Metallurgical Society of AIME, (1979), 145.
- [14] T. Sakaki, F. Sugimoto and T. Fukuzato: Acta Metall., 31(1983), 1737.
- [15] A. M. Sarosiek and W.S. Owen: Mater. Sci. Eng., 66(1984), 13.
- [16] N. K. Balliger and T. Gladman: Met. Sci., 15(1981), 95.
- [17] Y. Tomota: Mater. Sci. Technol., 3(1987), 415.
- [18] P. Uggowitzer and H. P. Stüwe: Mater. Sci. Eng., 55(1982), 181.